

## Enhanced efficiency of organic light-emitting devices with metallic electrodes by integrating periodically corrugated structure

Yan-Gang Bi,<sup>1</sup> Jing Feng,<sup>1,a)</sup> Yun-Fei Li,<sup>1</sup> Yu Jin,<sup>1</sup> Yue-Feng Liu,<sup>1</sup> Qi-Dai Chen,<sup>1</sup> and Hong-Bo Sun<sup>1,2,a)</sup>

<sup>1</sup>State Key Laboratory on Integrated Optoelectronics, College of Electronic Science and Engineering, Jilin University, 2699 Qianjin Street, Changchun 130012, China

<sup>2</sup>College of Physics, Jilin University, 119 Jiefang Road, Changchun 130023, China

(Received 2 December 2011; accepted 8 January 2012; published online 31 January 2012)

Photons trapped in form of surface-plasmon polariton (SPP) modes associated with the metallic electrode/organic interface results in a large energy loss in organic light-emitting devices (OLEDs). We demonstrate efficient outcoupling of SPP modes from one of two metal electrodes by integrating a periodic wavelength-scale corrugation into the device structure. 30% enhancement in efficiency has been obtained from the corrugated OLEDs with appropriate grating period. The efficient outcoupling of the SPPs has been verified by numerical simulations of both absorption spectra and field distribution. © 2012 American Institute of Physics. [doi:10.1063/1.3680595]

It is well-known that majority of the light generated in emissive layer is trapped in organic light-emitting devices (OLEDs) in form of waveguide (WG) modes in high refractive index indium-tin-oxide (ITO) anode layer and surface plasmon-polariton (SPP) modes associated with the metallic cathode/organic interface.<sup>1-3</sup> The low light outcoupling (less than 20%) has become one of the main limitations to high efficiency of the OLEDs. Using metallic anode, for example, thin metal film, metal grid, or metal nanowires with high optical transmission and electrical conductivity as a direct replacement for ITO has a potential to recover the power lost to the WG mode in ITO.<sup>4-6</sup> However, SPP modes exist at the cathode/organic interface is still a loss, which is up to about 40% in typical planar OLEDs based on small molecules.<sup>2,7</sup> Introducing a wavelength-scale microstructure at the metal surface has exhibited its remarkable effect for excitation and outcoupling of the SPP modes by providing an additional momentum to couple the SPP modes into light.<sup>8-12</sup> Therefore, improved light extraction would be expected by introducing a microstructure into the electrode of the OLEDs.

Although enhanced light extraction has been demonstrated by using microstructure previously,<sup>8</sup> outcoupling for the OLEDs with two metallic electrodes has not been thoroughly investigated. In this work, we report improved light extraction of OLEDs with metallic anode and periodic corrugation. Au thin film has been used in this work as anode instead of ITO due to not only its high conductivity and low absorbance across the visible range, but also the elimination of the microcavity effect usually persisted in normal OLEDs with two metallic electrodes. Moreover, the use of the Au instead of ITO as anode permits the elimination of the power lost to WG in ITO. The light trapped in SPP becomes the main power lost, which can be efficiently outcoupled by the introduction of the periodic corrugation into the device structure. The wavelength of SPP resonance at both anode and cathode/organic interfaces have been determined by both

experimentally measured and theoretically simulated absorption spectra, and has been tuned by adjusting the period of the corrugation to coincide with emitting wavelength of the OLEDs. The enhanced efficiency attributed to the excitation and outcoupling of SPP modes at the electrode/organic interface has been verified by the simulation of field distribution.

The periodic corrugation was fabricated on a photoresist layer spin-coated on the pre-cleaned glass substrates by a holographic lithography technique. The morphologies of the corrugation on the photoresist surface were characterized by an atomic force microscopy (AFM) as shown in Fig. 1(a). The grating amplitude was fixed at 70 nm by tuning the laser fluence. A 15 nm thick Au anode layer was deposited on the prepared substrates and then exposed in ultraviolet environment for 30 min in order to produce AuO<sub>x</sub> on the surface of Au film to reduce the hole-injection barrier.<sup>5</sup> The 25 nm thick hole injection layer of copper phthalocyanine (CuPc), 45 nm thick hole-transporting layer of N,N'-diphenyl-N,N'-bis(1,1'-biphenyl)-4,4'-diamine (NPB), 45 nm thick emitting layer of tris-(8-hydroxyquinoline) aluminum (Alq<sub>3</sub>), and cathode of Ca (2 nm)/Ag (100 nm) were deposited sequentially. Here, all layers were prepared by thermal evaporation in a high vacuum system with the pressure of  $5 \times 10^{-4}$  Pa. The AFM images of the surface morphologies of both deposited Au anode and Ag cathode layers were given in Figs. 1(b) and 1(c). The profile of the deposited layers was essentially a replication of the underlying photoresist, forming a periodic corrugation throughout the structure. The structure of the corrugated device is shown in Fig. 1(d). For comparison, a planar OLED was also fabricated on planar area of same photoresist coated substrates. The absorption spectra were measured by UV-VIS spectrophotometer (UV-2550, SHIMADZU). The angular dependent electroluminescent (EL) spectra were measured by fiber optic spectrometer. A slit was used to limit the angular acceptance to  $\sim 1^\circ$ , and the OLEDs were placed on a rotation stage with grooves parallel to the rotation axis. The current density-luminance characteristics were measured by Keithley 2400 programmable voltage-current source and Photo Research PR-655

<sup>a)</sup>Authors to whom correspondence should be addressed. Electronic addresses: jingfeng@jlu.edu.cn and hbsun@jlu.edu.cn.

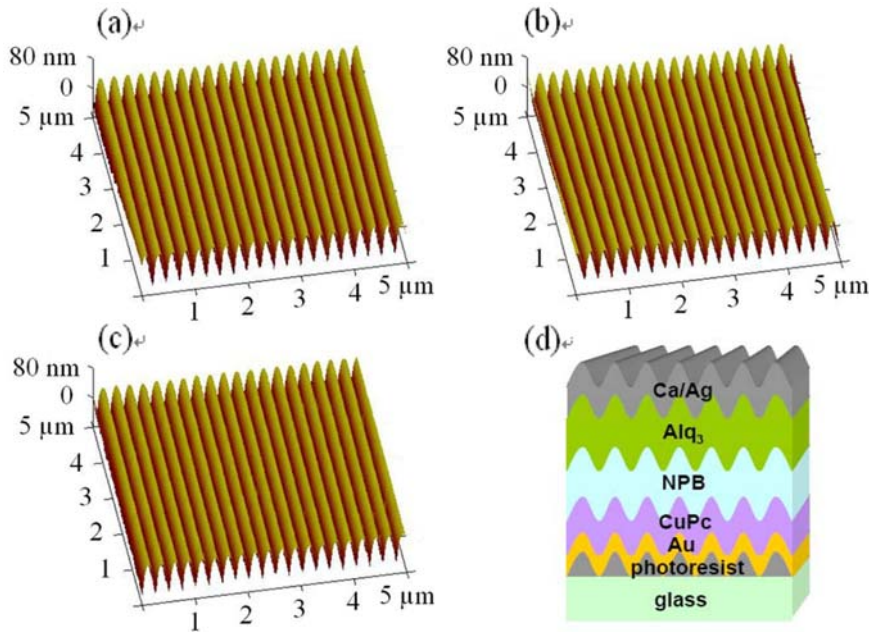


FIG. 1. (Color online) (a)-(c) AFM image of surface morphologies of corrugated photoresist, deposited Au anode and Ag cathode with 250 nm period on glass substrate. (d) Schematic structure of the corrugated OLED.

spectrophotometer. The active area of the device was  $2\text{ mm} \times 2\text{ mm}$ , and all of the measurements were conducted in air at room temperature.

SPP resonance at the corrugated metal surface can be tuned by adjusting the grating period. Its consistency with the emitting wavelength of the OLED is crucial for the efficient outcoupling of the SPP modes. First, both experimentally measurement and theoretically simulation of absorption spectra at normal direction are performed for the OLEDs with various grating period from 250 to 350 nm to determine the desired grating period. The thickness of the Ag cathode is decreased from 100 nm to 50 nm for the absorption measurement. A planar OLED was used as the reference sample for the absorption measurement of the corrugated OLEDs to exclude the absorption by the planar metal films and the CuPc at the observed wavelength region, so that the peaks originated from the SPP resonance supported by the periodic

corrugation can be distinguished clearly. In-house generated finite-difference time-domain (FDTD) code are applied to simulate the absorption spectra.<sup>11</sup> Two absorption maxima are observed, and exhibit blue shift with the decreasing grating period as shown in Figs. 2(a) and 2(b). The peak positions of the measured and simulated spectra agree with each other very well. One of the two absorption peaks for the 250 nm-corrugated device is at around 524 nm, which coincides with the emission peak of emitter (Alq<sub>3</sub>) employed in this device. In order to identify the two absorption maxima and establish the optical modes supported by the corrugated OLEDs, spatial steady-state  $H_z$  field intensity distribution of the transverse magnetic TM mode across the device structure as a function of position with the normal incident light has been calculated for the device with 250 nm grating period. The results of field distribution are shown in Figs. 2(c) and 2(d), corresponding to the two peak wavelength of 400 and

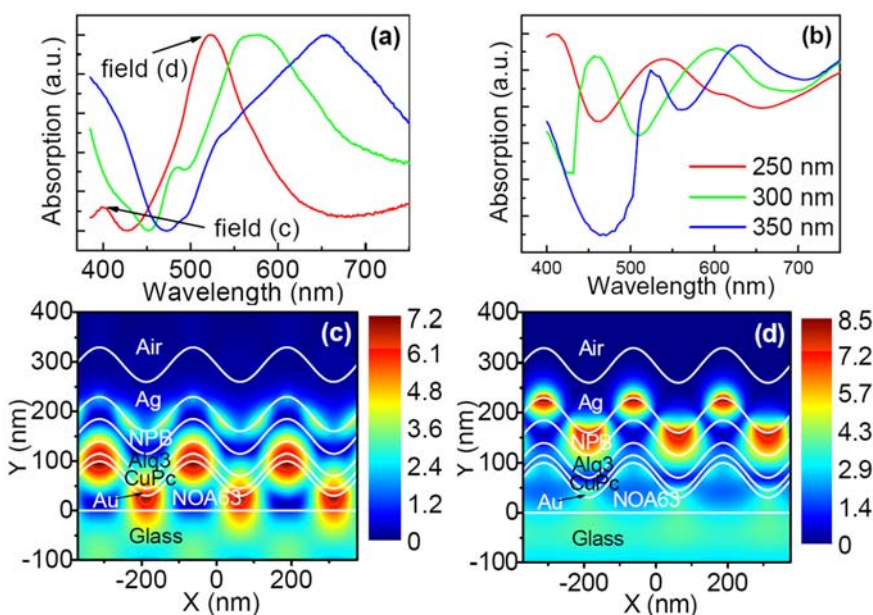


FIG. 2. (Color online) Experimentally measured (a) and theoretically calculated (b) absorption spectra with various period of corrugation. (c) FDTD simulated distribution of magnetic field intensity in the microstructured sample with 250 nm period at the wavelength of 400 and 524 nm, respectively.

524 nm observed from Fig. 2(a), respectively. The field intensity is with maximum at the Au/CuPc interface for the wavelength of 400 nm and at the Ag/Alq<sub>3</sub> interface for the wavelength of 525 nm, respectively, and decays along the direction perpendicular to it, which demonstrates that the absorption peaks originate from the SPP modes associated at the two electrode interfaces.<sup>13–15</sup> The longer wavelength one is from the SPP associated at the Ag electrode interface, and the shorter wavelength one is from the SPP associated at the Au anode interface. We should note that there is a difference in the peak intensity at the short wavelength between the experimental and simulated results. The measured peak intensity of the absorption associated at the Au interface is much lower compared to that of calculated results. The deposited Au film is only 15 nm, and surface smoothness and film continuity would be poor for such a thin film, which will limit the efficiency of the SPP resonance and reduce the measured absorption intensity at its interface.

We can conclude from the absorption spectra that 250 nm of grating period is favorable to extract the SPP modes at the Ag cathode/organic interface of the Alq<sub>3</sub>-based OLEDs because of its coincidence with the emitting peak of Alq<sub>3</sub>. EL maximum corresponding to the absorption peak should be observed if the optical modes are coupled out into far field radiation. Angular dependent EL spectra with TM polarization are measured from the OLEDs with 250 nm grating and compared with that of the measured absorption spectra to verify the outcoupling of the SPP modes, as shown in Figs. 3(a) and 3(b). The emission peak in both absorption and EL spectra splits into two peaks, and shifts in wavelength with increasing observation angle. Their peak wavelength is almost coincident, which demonstrates an efficient outcoupling of light from the trapped SPP modes, and an improved light extraction is expectable. The spectra shape

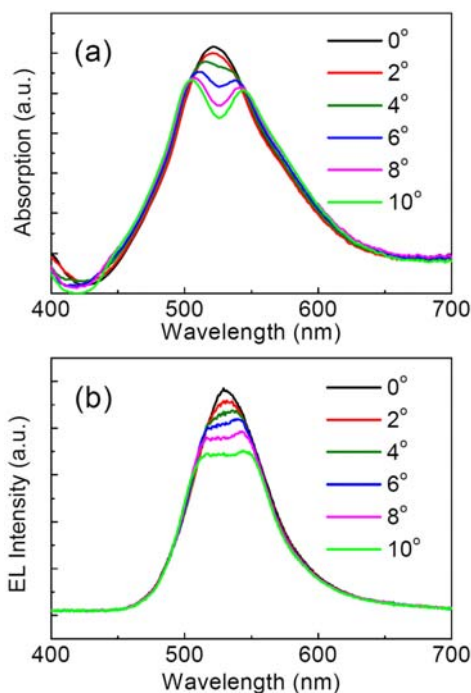


FIG. 3. (Color online) The angular dependent absorption (a) and EL (b) spectra from 0° to 16°.

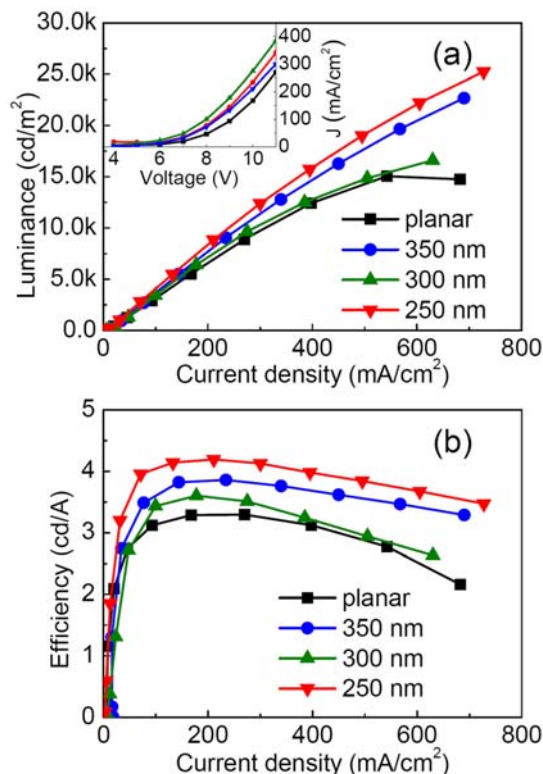


FIG. 4. (Color online) Luminance-current density (a) and efficiency-current density (b) characteristics of corrugated and planar OLEDs. The inset in (a) shows their voltage-current density characteristics.

between the absorption and EL emission show different, and a narrower bandwidth in the EL spectra is observed. This is because the fluorescence of the Alq<sub>3</sub> may decide the bandwidth of EL emission, while it has no influence on that of the absorption spectra.

The EL performances of the Alq<sub>3</sub>-based OLEDs with and without the corrugated structure are shown in Fig. 4. They show comparable current density at the same driving voltage, as shown in the inset of Fig. 4(a). The expected enhancement in both luminance and efficiency from the corrugated OLEDs is observed, which shows period dependence. The OLEDs with 250-nm grating period exhibit maximum EL performance. The maximum luminance is increased from 14750 to 25250 cd/m<sup>2</sup>. The maximum current efficiency is improved from 3.2 to 4.19 cd/A, which corresponds to a ~30% enhancement. This enhancement in EL efficiency confirms the above experimental and simulated results that the power lost to the SPP modes at the cathode/organic interface has been recovered as light in far field, which contributes to the much enhanced light extraction. The fraction of the power trapped in SPPs depends on the device structure, for example, the refractive index and the layer thickness of the materials employed in the devices.<sup>16,17</sup> In our case, the photons tapped in SPPs may not be extracted completely and further investigation is needed to optimize the device and the grating parameters to obtain a higher light extraction from the SPPs. It is possible to obtain a further improved light outcoupling by employing a microstructure with hexagonal or high order symmetry pattern due to its higher efficiency in coupling SPPs to far-field radiation.<sup>18,19</sup>

In summary, a periodic corrugation in wavelength-scale has been introduced into the bottom-emitting OLEDs with Au anode, and enhanced light extraction has been obtained. The introduction of the appropriate periodic corrugation has allowed the outcoupling of the SPP modes associated at the cathode/organic interface, which are usually trapped within planar devices, and results in a 30% enhancement in efficiency. Our results demonstrate that through the use of the periodic corrugation, power lost to the SPP modes can be recovered, thus opening an avenue to enhance the OLED efficiency.

The authors gratefully acknowledge the financial support from 973 project (2011CB013005) and NSFC (Grant Nos. 61177024, 60977025, and 61107024).

- <sup>1</sup>G. Gu, D. Z. Garbuzov, P. E. Burrows, S. Venkatesh, and S. R. Forrest, *Opt. Lett.* **22**, 396 (1997).  
<sup>2</sup>P. A. Hobson, S. Wedge, J. A. E. Wasey, I. Sage, and W. L. Barnes, *Adv. Mater.* **14**, 1393 (2002).  
<sup>3</sup>J. Hauss, T. Bocksrocker, B. Riedel, U. Geyer, U. Lemmer, and M. Gerken, *Appl. Phys. Lett.* **99**, 103303 (2011).  
<sup>4</sup>S. De, T. M. Higgins, P. E. Lyons, E. M. Doherty, P. N. Nirmalraj, W. J. Blau, J. J. Boland, and J. N. Coleman, *ACS Nano* **3**, 1767 (2009).

- <sup>5</sup>M. G. Helander, Z. B. Wang, M. T. Greiner, Z. W. Liu, J. Qiu, and Z. H. Lu, *Adv. Mater.* **22**, 2037 (2010).  
<sup>6</sup>P. Kuang, J. M. Park, W. Leung, R. C. Mahadevapuram, K. S. Nalwa, T. G. Kim, S. Chaudhary, K. M. Ho, and K. Constant, *Adv. Mater.* **23**, 2469 (2011).  
<sup>7</sup>L. H. Smith, J. A. E. Wasey, I. D. W. Samuel, and W. L. Barnes, *Adv. Funct. Mater.* **15**, 1839 (2005).  
<sup>8</sup>Y. Bai, J. Feng, Y. F. Liu, J. F. Song, J. Simonen, Y. Jin, Q. D. Chen, J. Zi, and H. B. Sun, *Org. Electron.* **12**, 1927 (2011).  
<sup>9</sup>S. Nien, N. Chiu, Y. Ho, J. Lee, C. Lin, K. Wu, C. Lee, J. Lin, M. Wei, and T. Chiu, *Appl. Phys. Lett.* **94**, 103304 (2009).  
<sup>10</sup>A. Fujiki, T. Uemura, N. Zettsu, M. A. Kasaya, A. Saito, and Y. Kuwahara, *Appl. Phys. Lett.* **96**, 043307 (2010).  
<sup>11</sup>X. L. Zhang, J. Feng, J. F. Song, X. B. Li, and H. B. Sun, *Opt. Lett.* **36**, 3915 (2011).  
<sup>12</sup>J. Feng, T. Okamoto, R. Naraoka, and S. Kawata, *Appl. Phys. Lett.* **93**, 051106 (2008).  
<sup>13</sup>W. L. Barnes, A. Dereux, and T. W. Ebbesen, *Nature* **424**, 824 (2003).  
<sup>14</sup>W. C. Liu and D. P. Tsai, *Phys. Rev. B* **65**, 155423 (2002).  
<sup>15</sup>C. J. Yates, I. D. Samuel, P. L. Burn, S. Wedge, and W. L. Barnes, *Appl. Phys. Lett.* **88**, 161105 (2006).  
<sup>16</sup>D. M. Koller, A. Hohenau, H. Ditlbacher, N. Galler, F. R. Aussenegg, A. Leitner, J. R. Krenn, S. Eder, S. Sax, and J. W. List, *Appl. Phys. Lett.* **92**, 103304 (2008).  
<sup>17</sup>S. Nowy, B. C. Krummacker, J. Frischeisen, N. Reinke, and W. Brütting, *J. Appl. Phys.* **104**, 123109 (2008).  
<sup>18</sup>A. A. Letailleur, K. Nomenyo, S. M. Murtry, E. Barthel, E. Søndergård, and G. Lérondel, *J. Appl. Phys.* **109**, 016104 (2011).  
<sup>19</sup>P. T. Worthing and W. L. Barnes, *Appl. Phys. Lett.* **79**, 3035 (2001).